



Utilizing Machine Learning Models with Limited Meteorological Data as Alternatives for the FAO-56PM Model in Estimating Reference Evapotranspiration

Shima Amani¹ · Hossein Shafizadeh-Moghadam¹ · Saeid Morid¹

Received: 4 September 2023 / Accepted: 13 November 2023 / Published online: 7 February 2024
© The Author(s), under exclusive licence to Springer Nature B.V. 2024

Abstract

The current study evaluated the accuracy of four machine learning (ML) models and thirteen experimental methods calibrated to estimate reference evapotranspiration (ET_0) in arid and semi-arid regions. Various scenarios were examined utilizing meteorological data and FAO56-PM as a benchmark. According to the results, the ML models outperformed the experimental methods on both daily and monthly scales. Among the ML models, artificial neural networks (ANNs), generalized additive model (GAM), random forest (RF), and support vector machine (SVM), respectively, demonstrated higher accuracy on a monthly scale, while ANNs, SVM, RF, and GAM exhibited greater accuracy on a daily scale. Notably, ANNs and SVM achieved high accuracy even with a limited number of variables. Conversely, RF showed improved accuracy with an increased number of variables. Comparing the ML and experimental models with equivalent inputs revealed that ANN with inputs similar to Valiantzas-1 performed better on a monthly scale, while SVM with inputs akin to Valiantzas-3 showed superior performance on a daily scale. Our findings suggest that average temperature, wind speed, and sunshine hours contribute significantly to the accuracy of ML models. Consequently, these ML models can serve as an alternative to the FAO56-PM method for estimating ET_0 .

Keywords Reference evapotranspiration · FAO-56PM · Machine learning · Experimental models

1 Introduction

Efficient management of water resources in the agricultural sector is crucial for mitigating water crises (Lu et al. 2023; Roy et al. 2023), particularly in arid and semi-arid regions. Iran allocates over 90% of its water resources to agriculture (Alizadeh and

✉ Hossein Shafizadeh-Moghadam
h_shafizadeh@modares.ac.ir

Shima Amani
Sh_amani@modares.ac.ir

Saeid Morid
morid_sa@modares.ac.ir

¹ Department of Water Engineering and Management, Tarbiat Modares University, Tehran, Iran

Keshavarz 2005; Fathi-Taperasht et al. 2022). Evapotranspiration (ET) plays a vital role in optimizing water demand in agriculture, as more than 90% of the water utilized in agricultural ecosystems is lost through ET (Shan et al. 2020; Wang et al. 2019). ET also constitutes a basis for various calculations in water resources management as well as in the design and operation of irrigation and drainage systems (Feng et al. 2017; Yan et al. 2023). Accurate estimation of ET at the field level can greatly enhance management planning for irrigation water, determining the irrigation cycle, estimating the hydromodule of the network (water demand of crops), and predicting crop yield (Allen et al. 1998; Bachour et al. 2016; Anderson et al. 2007; Teuling et al. 2009).

Various factors influence ET variations, a complex physical phenomenon comprising multiple nonlinear processes (Jovic et al. 2018; Li et al. 2022; Amani and Shafizadeh-Moghadam 2023). Over the years, researchers have proposed two general groups of ET measuring techniques: point methods and regional methods. Lysimeter, a point method, is used to measure ET directly with no assumptions (Holmes 1984) and is a benchmark for calibrating other methods (Liu et al. 2017). Nevertheless, its limited availability, high costs, operational challenges, and environmental impact restrict its usage (Fan et al. 2018; WMO 1963; Scanlon et al. 1997). As a result, mathematical models that utilize meteorological data to estimate ET have gained popularity (Ferreira et al. 2019), and numerous indirect methods for estimating ET based on influential factors have been developed (Almorox et al. 2015). The Penman–Monteith (PM) model modified by the Food and Agriculture Organization (FAO) is widely used as a reference for evaluating the performance and calibration of other ET estimation models (Allen et al. 1998).

The FAO56-PM model requires a complete set of meteorological data, comprising air temperature (maximum temperature (T_{max}), minimum temperature (T_{min}) and average temperature (T_m)), relative air humidity (RH), net solar radiation (R_n), wind speed (W_s), atmospheric pressure, and soil heat flux (G). However, the cost of collecting this data is considerable not only in developed countries (Chu et al. 2017), but also and most particularly in developing countries. Consequently, reliable data may not be consistently available over consecutive years (Bellido-Jiménez et al. 2021; De Paola and Giugni 2013; Eccel 2012). Therefore, preferred over the FAO56-PM model are alternative experimental methods, the most common of which are categorized as temperature-based methods that utilize T_{max} and T_{min} (Hargreaves and Samani 1985; Hargreaves et al. 1985; Blaney and Criddle 1962), solar radiation-based methods that use the difference between R_n , G , and latent heat (λ) (Abtew 1996; Irmak et al. 2003; Makkink 1957; Priestley and Taylor 1972), mass transfer-based methods that employ Dalton's law and the concept of water vapor flux transfer (Penman 1948; WMO 1963), and hybrid methods that combine various parameters such as solar radiation (R_s), T (T_m , T_{max} , T_{min}), and RH (Doorenbos and Pruitt 1977; Valiantzas 2013a, b). These methods are often complex, nonlinear, influenced by random factors, and rely on multiple assumptions. Each method is optimized based on the specific characteristics and unique weather conditions of the area under study (Küçüktopcu et al. 2023). Experimental methods for measuring ET, however, are limited to field or catchment-level applications. Furthermore, their results are dependent on time and location, hindering generalization of the findings to other areas. The need to calibrate equation coefficients and the inherent uncertainty associated with these methods have further contributed to their limitations (Islam and Alam 2021; Kisi et al. 2015).

The inherent nonlinearity and instability of meteorological variables makes challenging the complex phenomenon of ET estimation. Consequently, developing a precise physics-based formula for making accurate estimations is difficult. Thus, researchers have recently

turned their attention to machine learning (ML) as an alternative approach for ET estimation (Krishnashetty et al. 2021). Numerous studies have demonstrated that ML techniques such as artificial neural networks (ANNs), support vector machines (SVMs), and random forest (RF) outperform empirical and semi-empirical methods in estimating reference evapotranspiration (ET_0). ML methods offer advantages such as fast computation, high accuracy, and strong generalization capability (Elbeltagi et al. 2021; Feng et al. 2016; Mousavi et al. 2015; Abd-Elaty et al. 2023). Kumar et al. (2002) introduced an ANN for calculating ET_0 that exhibited accuracy comparable to the FAO-56 PM method. Shi et al. (2020) investigated daily ET_0 in southeastern Australia and demonstrated the superior performance of RF over empirical equations. Rahimi Khoob (2008) developed an ANN model based on the Hargreaves method that used monthly data from the Khuzestan Plain of Iran, and it outperformed the Hargreaves model. Tabari et al. (2012) simulated ET_0 in Iran utilizing several ML methods, all of which outperformed the Blaney-Criddle, Hargreaves, and Jensen Haise models. Landeras et al. (2018) found that ANN models outperformed the Hargreaves method when using the same inputs. Rashid Niaghi et al. (2021) simulated ET_0 in a semi-humid climate using gene expression programming (GEP), SVM, ML, and RF methods with empirical equations as inputs. They found that the combination of radiation-based models and the RF model yielded the best performance results across all stations.

Evaluating ML models to reduce input data is crucial because of the significance of data availability in estimating ET. Wen et al. (2015) employed SVM and ANN to model ET_0 using limited meteorological data in arid regions of China and compared their results with experimental models like those of Priestly-Taylor and Hargreaves. They found that SVM performed best when using T_m , R_s , and W_s data. Mohammadrezapour et al. (2018) investigated the performance of SVM, adaptive neuro-fuzzy inference system (ANFIS), and GEP utilizing five combinations of inputs to simulate ET_0 in southeast Iran from 1970 to 2010 and found that SVM performed superiorly with inputs consisting of T_m , RH, W_s , and sunshine hours (Sshn). Ferreira et al. (2019) evaluated the performance of ANN and SVM models in estimating ET_0 across Brazil using either T_m and RH data or T (T_{min} , T_m , T_{max}) alone; both models demonstrated acceptable accuracy. Bellido-Jiménez et al. (2021) developed various neural intelligence methods, including MLP, generalized regression neural network (GRNN), extreme learning machine (ELM), SVM, and RF, to estimate ET_0 using temperature-based data as the only input in southern Spain. They concluded that ELM performed superiorly in all scenarios and locations. In general, ML models using fewer inputs exhibit comparable performances to the FAO-56PM model and outperform experimental methods.

Although ML models excel at unraveling intricate relationships, their effectiveness as data-driven models depends on the careful selection of variables, data quality, and the optimization of model parameters. Determining these parameters, however, typically depends on user expertise and the nature of the input data. In ET estimation, one approach for selecting ML variables is to align them with the inputs used in experimental methods. Despite numerous studies having explored ET estimation using different variables, few have compared ML models to experimental methods for estimation accuracy, identification of important variables, and the generalizability and stability of results. In the current study, 13 experimental methods and four ML models were examined to estimate ET_0 in a watershed located in southwestern Iran. The study objectives were: 1) to compare the accuracy of ML and experimental models with similar inputs, 2) to assess the accuracy of ML models compared to the FAO56-PM model using minimal input data, and 3) to identify the variables that influence ET.

2 Material and Methods

2.1 General Methodology

Figure 1 depicts a flowchart illustrating the primary steps of this study. Initially, annual precipitation was processed to identify wet, drought, and normal years. Next, meteorological data for these periods were gathered and utilized as input for estimating ET_0 using FAO-56PM, experimental models, and ML models. The results were then assessed using three indices: R^2 (coefficient of determination), RMSE (root mean square error), and MAE (mean absolute error).

2.2 Study Area

The current study considered the Karkheh Basin located in the southwest of Iran. Covering an area of 51,000 km², the basin originates from the Zagros mountain range, flows into Horul Azim (Fig. 2), and boasts elevations varying from 3626 (m.a.s.l) in upstream regions to -8 (m.a.s.l) in downstream areas. The upper parts of the basin are characterized as semi-arid, while the southern part is classified as dry. Average precipitation in the region measures 474 mm and daily T_m fluctuate between -13.7 and 45.9 °C. Dam construction and the expansion of agricultural lands, particularly irrigated areas, have been an enduring characteristics of this basin.

2.3 Wet, Drought, and Normal Year Selection

Meteorological data from 15 stations within the Karkheh Basin were procured from the National Meteorological Organization of Iran. Table S1, provided in the supplementary file, provides the main characteristics of the data. Precipitation data for the years 2000 to 2021 were analyzed. Average annual precipitation (\pm SD) was calculated and the mean \pm 1SD was derived. Wet and drought years were defined as average annual precipitation exceeding the mean \pm 1SD average precipitation lower than the mean-1SD, respectively; those

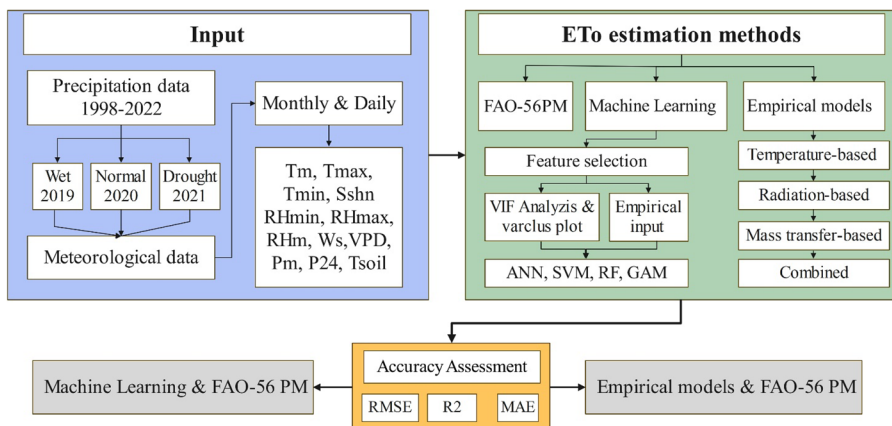


Fig. 1 General Methodology

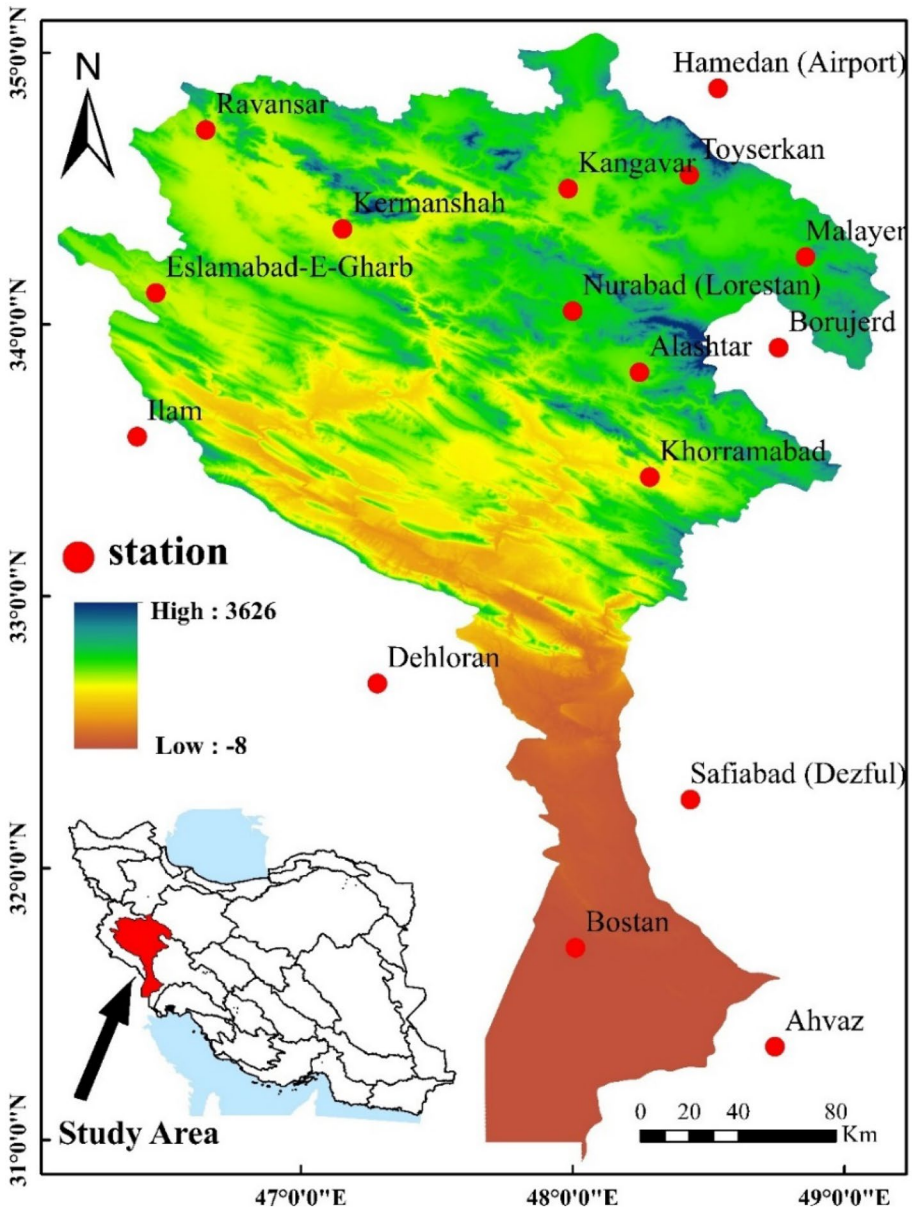


Fig. 2 Study area and its location in Iran

years falling within these two intervals were considered normal (Chow et al. 1971; McCuen 2016). Thirteen stations reported drought conditions in 2019, eight experienced normal conditions in 2020, and 12 encountered drought in 2021.

2.4 ET Estimation Models

2.4.1 FAO56-PM

The effectiveness of 13 experimental and four ML models was evaluated using the PM equation, specifically the FAO56-PM model (Eq. 1), as the benchmark and calculated as (Allen et al. 1998):

$$ET_0 = \frac{0.408\Delta}{\Delta + \gamma} (R_n - G) + \frac{\gamma}{\Delta + \gamma} \frac{\frac{900}{(T_a + 273)} u_2 (e_s - e_a)}{(1 + 0.34u_2)} \quad (1)$$

where ET_0 denotes reference evapotranspiration (mm/day), R_n is the net solar radiation at the crop surface ($\text{MJ m}^{-2} \text{d}^{-1}$), G represents soil heat flux ($\text{MJ m}^{-2} \text{d}^{-1}$) (which is typically ignored for daily estimates), T_a indicates the daily mean air temperature ($^{\circ}\text{C}$), u_2 represents the wind speed at a height of 2 m (m s^{-1}), e_s signifies the saturation vapor pressure (kPa), e_a represents the actual vapor pressure (kPa) (obtained using maximum and minimum relative humidity), Δ indicates the slope of the vapor pressure curve ($\text{kPa } ^{\circ}\text{C}^{-1}$), and γ denotes the psychrometric constant ($\text{kPa } ^{\circ}\text{C}^{-1}$).

2.4.2 Experimental Methods

The 13 experimental models utilized to estimate ET_0 were the Hargreaves-Samani and Blaney-Criddle (temperature-based); Penman and WMO (mass transfer-based); Makkink, Priestley-Taylor, Jensen-Haise, Abtew, and Irmak (radiation-based); and the Doorenbos-Pruitt, Valiantzas-1, Valiantzas-2, and Valiantzas-3 (combined approaches) models. These models were specifically developed to cater to diverse climatic conditions and geographical regions. Table 1 presents the equations and references for these experimental models.

2.4.3 Machine Learning Models

Random Forest RF, a tree-based model introduced in 2001 (Breiman 2001), was developed using a base learner called CART which has the capability to model nonlinear and complex patterns (Hastie et al. 2009). Unlike CART which can yield significantly different trees with minor variations in input data, RF employs the bootstrapping sampling method and generates multiple data samples using replacements from the original dataset. Each sample is then used to train a CART model, and the final output is determined by averaging the results. This ensemble approach produces more stable outcomes than CART (Carter and Liang 2019).

Artificial Neural Networks Multiple ANNs with different architectures have been developed for various applications; among them, the multilayer perceptron is widely utilized. Regardless of the architecture, a learning algorithm is employed to discover the relationships between independent and dependent variables. The learning process entails adjusting the weights to minimize prediction error. During the ANN training phase, the learning algorithm optimizes the weights by reducing the prediction error through a repetitive procedure called backpropagation, which computes the difference between the predicted and the actual output of the network (Rumelhart et al. 1986). The direction and magnitude of the weight adjustments are determined by the partial derivative of the error with respect to each weight (Hecht-Nielsen 1992).

Table 1 Experimental models for estimating reference evapotranspiration

NO	Models	Equations	References
Temperature-based			
1	Hargreaves–Samani	$ET_{Hs} = [0.0023 \times Ra \times (Tave + 17.8) \times (Tmax - Tmin)^{0.517}] / \lambda$	Hargreaves and Samani 1985
2	Blaney–Criddle	$ET_{BC} = a + bP(0.46T + 8.13)(1 + 0.0001H)$	Blaney and Criddle 1962
Radiation-based			
3	Makkink	$ET_{Ma} = 0.7 \frac{\Delta}{\Delta + \gamma} \frac{R_s}{\lambda}$	Makkink 1957
4	Jensen–Haise	$ET_{JH} = (0.025T + 0.08)R_s$	Jensen and Haise 1963
5	Abtew	$ET_{Ab} = 0.01786 \frac{R_s \times T_{max}}{\lambda}$	Abtew 1996
6	Priestley–Taylor	$ET_{PT} = 1.26 \frac{\Delta}{\Delta + \gamma} \frac{Rn - G}{\lambda}$	Priestley and Taylor 1972
7	Irmak	$ET_{Ir} = 0.149R_s + 0.079T - 0.611$	Irmak et al. 2003
Mass transfer-based			
8	Penman	$ET_{pe} = 0.35 \left(1 + \frac{0.98}{100u_2} \right) (e_s - e_a)$	Penman 1948
9	WMO	$ET_{wm} = (0.1289 + 0.034u_2)(e_s - e_a)$	WMO 1963
Combined			
10	Valianzas1	$ET_{V1} = 0.0393R_s - \sqrt{T + 9.5} \times 0.19R_s^{0.6} \phi^{0.15} + 0.078(T + 20) \left(1 - \frac{RH}{100} \right)$	Valiantzas 2013a, b
11	Valianzas2	$ET_{V2} = 0.0393R_s - \sqrt{T + 9.5} \times 0.19R_s^{0.6} \phi^{0.15} + 0.0061(T + 20)(1.12T - Tmin)^{0.7}$	Valiantzas 2013a, b
12	Valianzas3	$ET_{V3} = 0.0393R_s - \sqrt{T + 9.5} \times 0.19R_s^{0.6} \phi^{0.15} + 0.078(T + 20) \left(1 - \frac{RH}{100} \right) \times u_2^{0.7}$	Valiantzas 2013a, b
13	Doorenbos&Pruitt	$ET_{DP} = \left[\frac{\Delta}{\Delta + \gamma} (Rn - G) + 2.7 \frac{\Delta}{\Delta + \gamma} \frac{(1 + 0.86u_2)}{\lambda} (e_s - e_a) \right]$	Doorenbos and Pruitt 1977

Ra extraterrestrial radiation (MJ m⁻² d⁻¹), *Rs* solar radiation (MJ m⁻² d⁻¹), *Rn* the net solar radiation (MJ m⁻² d⁻¹), *T*, *Tmax*, and *Tmin* are mean, maximum, and minimum temperature (°C), respectively, *u₂* wind speed at a height of 2 m (m·s⁻¹ in all equations except for the Penman model, where *u₂* is measured in miles d⁻¹), *es* saturation vapor pressure (hPa in all equations, except for the Penman model, where *es* is in mmHg), *ea* actual vapor pressure (hPa in all equations, except for the Penman model, where *ea* is in mmHg), *RH* relative humidity (expressed as a percentage), *a* = 0.0043 (RHmin) - *n/N* - 1.41, *b* = 0.82 - 0.0041 (RHmin) + 1.07 (*n/N*) + 0.06 (U2) - 0.006 (RHmin) (*n/N*) - 0.0006 (RHmin) (U2), Δ slope of the vapor pressure curve (kPa °C⁻¹), γ psychrometric constant (kPa °C⁻¹), λ latent heat of vaporization (2.45 MJ kg⁻¹), *G*: soil heat flux density (MJ m⁻² d⁻¹), and ϕ latitude (radians)

Support Vector Machine SVM performs well when the available training data is limited (Mantero et al. 2005). This algorithm maps each data instance onto an n -dimensional space, where the dimensions represent the features or independent variables, and then separates them using a line or plane (Cortes and Vapnik 1995). In certain cases, separation is improved by transforming the samples to a higher-dimensional space using kernels. Commonly employed kernels include sigmoid, linear, radial basis function (rbf), and polynomial ones. The support vector acts as an optimal boundary that effectively separates the data groups, aiming to maximize the margin with the data.

Generalized Additive Model GAM is suitable for situations in which the relationship between independent variables and the response variable is complex and non-linear, such as in environmental processes. GAM is a non-parametric extension of a generalized linear model (Hastie and Tibshirani 1990) that offers explicit insight into the relationships between variables. It allows the response curve to be determined by the observed data utilizing splines, i.e., mathematical functions that offer flexibility in fitting intricate curves to the data. Splines divide the curve into smaller, simpler segments, enabling the representation of the non-linear relationship between independent variables and the response variable (Hastie and Tibshirani 1990).

2.4.4 Variable Selection for ET Estimation

The efficacy of ML models can be affected by the existence of collinearity among independent variables. In this research, collinearity among variables was examined daily and monthly and input variables were selected using variable clustering and variance inflation factor (VIF). Variable clustering is advantageous in feature selection, as it allows for the identification of representative variables within each cluster, which can then be chosen for subsequent analysis or modeling purposes. VIF quantifies the degree of multicollinearity; a VIF value of 1 indicates no collinearity, while a value exceeding 5 is considered indicative of high multicollinearity (O'Brien 2007).

2.5 Model Evaluation

RMSE, MAE, and R^2 (Eqs. 2–4) were used to assess the performance of both experimental and ML models. RMSE indicates an overall measure of the error, MAE indicates the average absolute error, and R^2 indicates the relationship between the observed and predicted values. R^2 should be as close to one as possible, and RMSE and MAE should be close to zero.

$$RMSE = \sqrt{\frac{\sum_1^N (P_i - Q_i)^2}{N}} \quad (2)$$

$$R^2 = \frac{\sum_1^N (Q_i - Q_{avg})(P_i - P_{avg})}{\sqrt{\sum_1^N (Q_i - Q_{avg})} \sqrt{\sum_1^N (P_i - P_{avg})}} \quad (3)$$

$$MAE = \frac{\sum_1^N (P_i - Q_i)}{n} \quad (4)$$

where P_i is the predicted value of ET_0 , P_{avg} represents the predicted mean ET_0 , Q_i denotes the observed value, Q_{avg} shows the mean observed ET_0 , and n is the number of data.

3 Results and Discussion

3.1 Evaluation of Experimental Models

Different experimental models based on FAO56-PM were assessed using daily and monthly data for normal, drought, and wet years. The combined models exhibited higher accuracy on both daily and monthly scales (Figs. 3 and 4). Conversely, the mass transfer-based models displayed low accuracy. The temperature-based Blaney-Criddle method showed superior accuracy on both daily and monthly scales, potentially because of its incorporation of *Ws* in the calculation of constants *a* and *b*. Among the radiation-based models, the Abtew method (RMSE: 0.78, R^2 : 0.93 and MAE: 0.57) and Priestley-Taylor (RMSE: 1.57, R^2 : 0.90 and MAE: 1.17) achieved the highest and lowest accuracy, respectively on a monthly scale. On a daily scale, Priestley-Taylor was the most accurate (RMSE: 1.41, R^2 : 0.79 and MAE: 1.02), whereas the Jensen-Haise model was the least accurate (RMSE: 8.81, R^2 : 0.88 and MAE: 6.85). In the combined models, the Valiantzas-3 method demonstrated

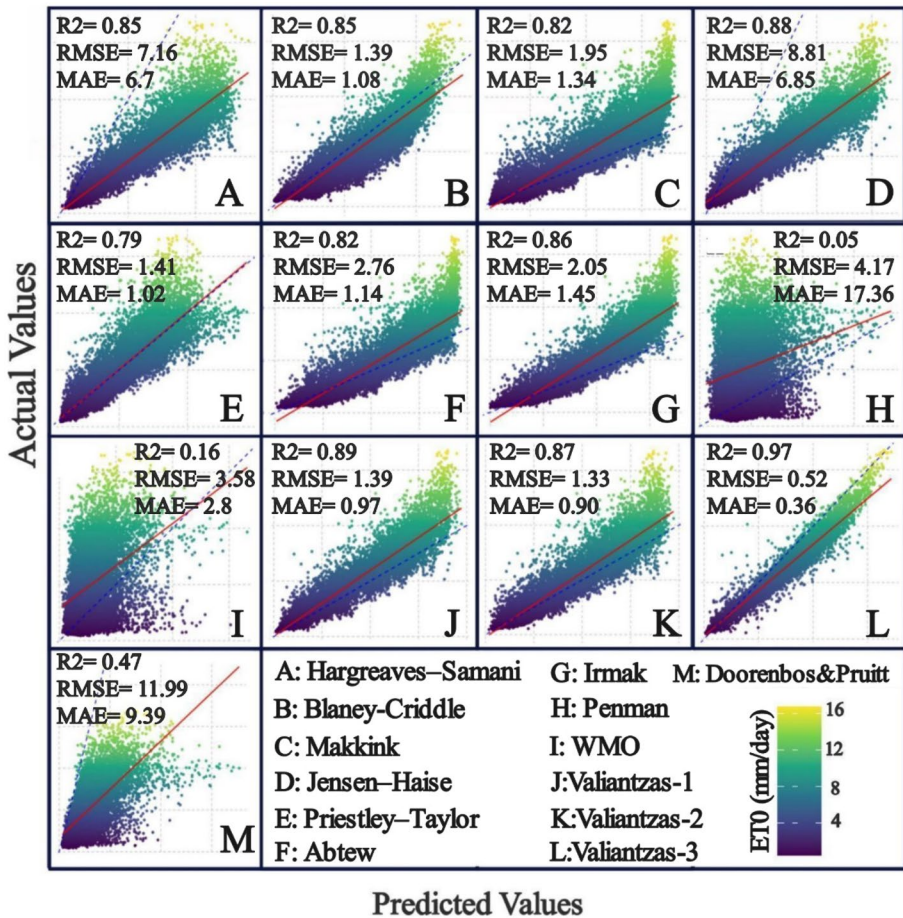


Fig. 3 Experimental models for estimating ET_0 at the daily interval

the highest accuracy, while Doorenbos and Pruitt’s method exhibited the lowest accuracy on both daily and monthly scales. According to Fig. 4, the Valiantzas-3 and -1, Abtew, Makkink, and Jensen-Haise models showed higher monthly accuracy compared with other methods, while the Valiantzas-3, Blaney-Criddle, Valiantzas-2, and Priestley-Taylor models showed the most accuracy on a daily scale. The experimental models performed differently across various time scales. Because Valiantzas-3 and Valiantzas-1 required W_s and RH, the Abtew and Makkink models which require the least input were selected for the monthly scale. The Valiantzas-2 and Priestley-Taylor models were found to be most suitable for the daily scale, because Valiantzas-3 and Blaney-Criddle models incorporate W_s in their inputs.

Figure 4 presents a performance comparison between the FAO56-PM and various experimental models on the daily scale. As illustrated, the Valiantzas-3, Blaney-Criddle, Valiantzas-2, and Priestley-Taylor models exhibited superior performances for daily ET_0 estimation compared to the other models for daily, and thus, the Valiantzas-2 and Priestley-Taylor models were considered the optimal choices. Figures 3 and 4 show the results from evaluations of 13 experimental models on daily and monthly scales, respectively. Among

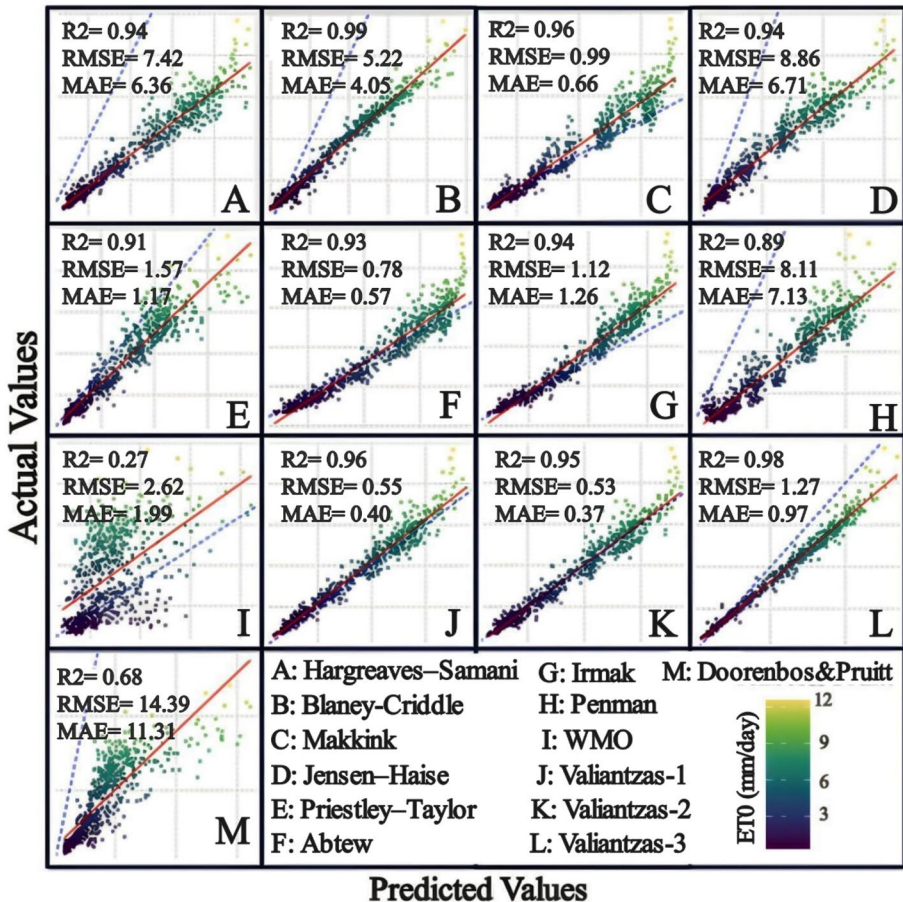


Fig. 4 Experimental models for estimating ET_0 at the monthly interval

Table 2 Variable selection using VIF

VIF Analyzis		Daily	Monthly
Removed			
thresh	10	Tmax, Tm, RHm	Tm, Tmax, Tmin, RHm
	5	Tm, Tmax, Tmin, RHm	Tm, Tmax, Tmin, RHm, Sshn
	3	Tm, Tmax, Tmin, RHm, Rhmin	Tm, Tmax, Tmin, RHm, Sshn

these models, the Valiantzas-3, Valiantzas-1, and Abtew models demonstrated superior performances on the monthly scale. The Abtew model utilizes RS and Tmax as inputs, while the Valiantzas-1 model incorporates Rs, Tm, and RH as inputs. As the model requiring the minimum monthly ET₀ data, Abtew was deemed more suitable. It also benefits from a simpler equation.

3.2 Variable Selection for Machine Learning Models

Based on VIF analysis, Ws, vapor-pressure deficit (VPD), and Sshn demonstrated the least collinearity (Table 2); however, why temperature was excluded from the daily and monthly scales is inexplicable, considering its crucial role in ET estimation. The results were further investigated using the variable clustering method, and Fig. 5 presents the outcomes, where one variable from each group falling below the 0.8 dashed line should be chosen. Tm was selected from the group of variables (Tsoil, Tm, Tmax, Tmin), because Tmin and Tmax only represent specific times of the day and cannot adequately capture the Tm for water consumption throughout the entire day. Furthermore, measuring Tmin and Tmax may require specific instruments that are not universally available. Average relative humidity (RHm) was chosen from the group of relative humidity variables (RHm, minimum relative humidity (RHmin), maximum relative humidity (RHmax)), because it reflects the capacity of air to hold water vapor, and higher relative humidity indicates a closer proximity to saturation, resulting in lower ET. Rhmax represents the maximum relative humidity recorded during the day or month, leading to a lower estimation of ET. Conversely, RHmin causes overestimation. VPD was selected

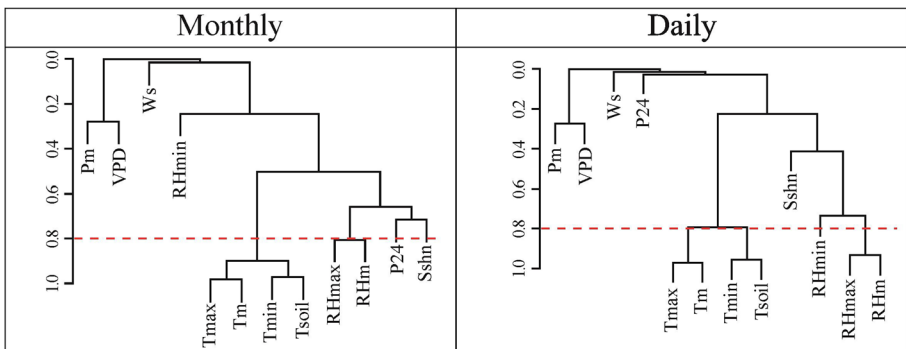


Fig. 5 Variable selection using the variable clustering method

Table 3 Combinations of input variables for ET estimation using ML models

NO	Variabel	NO	Variabel
1	Tm, Ws	7	Tm, Ws, Sshn, VPD
2	Tm, RH	8	Tm, Sshn, RHm, VPD
3	Tmax, Tmin	9	Tm, RHm, Ws, VPD
4	Tm, Ws, Sshn	10	Ws, Sshn, RHm, VPD
5	Tm, Ws, RHm	11	Tm, Ws, Sshn, RHm, VPD
6	Ws, VPD, Sshn	12	All Variabels

from the group (VPD and mean pressure (Pm)), as it directly indicates the atmosphere’s ability to accept water vapor. Based on theoretical considerations and the results of both methods, Tm, RHm, VPD, Sshn, and Ws were chosen for modeling ET estimation.

Apart from selecting variables statistically, the availability, low cost, and measurement accuracy of each variable must also be considered. Therefore, various combinations were explored for ET estimation (Table 3). Furthermore, to compare the outputs of the ML models and experimental methods, the input variables of experimental methods were also examined to be used as input for ML models.

3.3 ML Models for ET Estimation

The current study assessed the use of RF, SVM, ANN, and GAM models for estimating ET using different combinations of input variables. The findings are presented in three sections: models utilizing input data similar to the FAO56-PM, models employing diverse input combinations, and models incorporating inputs similar to the experimental methods.

3.3.1 ML Models for ET Estimation Using the Same Input as FAO56-PM

Figure 6 shows the performance comparison of RF, SVM, ANN, and GAM models on daily and monthly scales using the same inputs as the FAO56-PM model. As seen, all

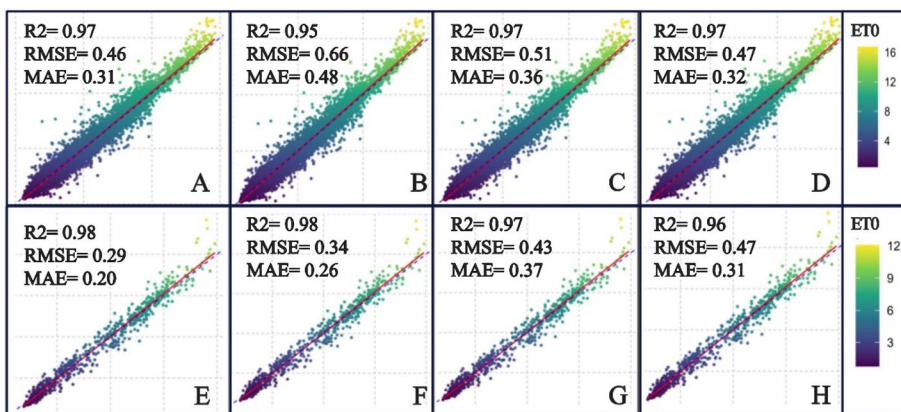


Fig. 6 ET estimation using the ML models **A:** ANN daily, **B:** GAM daily, **C:** RF daily, **D:** SVM daily, **E:** ANN monthly, **F:** GAM monthly, **G:** RF monthly, and **H:** SVM monthly

models achieved high accuracy with performances similar to that of the FAO56-PM model. Nevertheless, ML models required a significantly longer computational time than the FAO56-PM model using software such as CropWat or Macro Excel. All ML models were executed in less than a minute, and the most accurate models for monthly and daily scales were ANN and SVM, respectively.

3.3.2 ML Models for ET Estimation Using Different Input Combinations

Figure 7 illustrates the results of ML models utilizing various combinations of inputs as presented in Table 4. Overall, both R^2 and RMSE values improved as more inputs were included, with the ANN model consistently outperforming other models across most combinations. ANN, GAM, RF, and SVM, respectively, exhibited higher accuracy when predicting on a monthly scale. When estimating on the daily scale, however, ANN, SVM, RF, and GAM were respectively more precise.

In terms of two-variable combinations, the ANN model incorporated T_m and W_s and demonstrated the highest accuracy for daily predictions. For monthly predictions, the SVM utilizing T_m and W_s as well as the GAM employing W_s and VPD exhibited superior accuracy. These findings suggest the importance of W_s in estimating ET. By adding S_{shn} to the T_m and W_s , an accuracy very close to that of the models with all inputs was achieved by SVM on the monthly scale and ANN on the daily scale. Models using four variables achieved similar accuracy to models using all variables. Among different combinations, adding RH or VPD had an equivalent effect on the combination set of T_m , W_s , and S_{shn} , which is in line with the findings of Mohammadrezapour et al. (2018). Furthermore, by introducing S_{shn} to the T_m and W_s variables in the subsequent combination, a level of accuracy comparable to that of models employing all inputs was achieved. The SVM and ANN models displayed greater accuracy for monthly and daily predictions, respectively.

To summarize, ANN and SVM demonstrated superior performances when utilizing a smaller number of variables, whereas RF exhibited better results when incorporating a larger number of variables. T_m , W_s , and S_{shn} were identified as influential factors in enhancing the accuracy of the ML models. Consequently, models incorporating these three inputs can serve as a viable alternative to the FAO-56PM method. Fan et al. (2019) discovered that including solar radiation further improved the accuracy of the models, and Pandey et al. (2016) demonstrated that models utilizing W_s data achieved higher levels of accuracy.

3.3.3 ML Models for ET Estimation Using the Same Input as Experimental Models

The findings of a comparison between ML models and experimental methods using the same input variables showed that ML models surpassed all experimental models in accuracy for both daily and monthly scales, as shown in Table 5. Specifically, the ANN employing identical inputs as Valiantzas-1 demonstrated a superior performance on the monthly scale, while the SVM utilizing the same inputs as Valiantzas-3 exhibited better results on the daily scale. As mentioned in the preceding section, the Valiantzas-2 and Priestley-Taylor models were determined to be appropriate for daily scale estimations, while the Abteu model was found to be suitable for monthly scale estimations. Among the ML models, the SVM aligned with the Priestley-Taylor model and the RF aligned

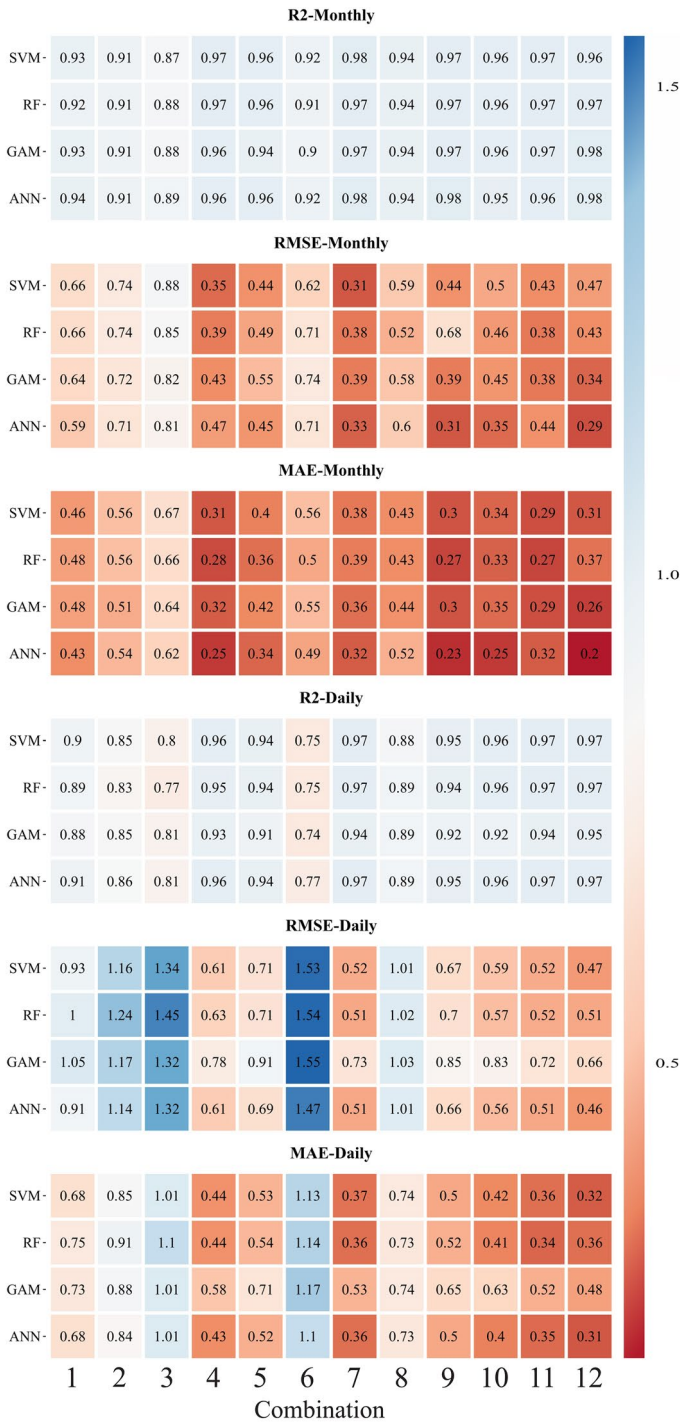


Fig. 7 Accuracy of ML models for ET estimation using different input combinations

Table 4 Accuracy of the ML models with variables similar to the experimental models

Models	Models Input	R ²	RMSE	MAE	R ²	RMSE	MAE
		Monthly			Daily		
Temperature-based							
Hargreaves–Samani	Ra, Tm, Tmax, Tmin	0.94	7.42	6.36	0.85	7.16	6.07
RF	Tmax, Tmin, Tm	0.90	0.78	0.6	0.83	1.26	0.94
SVM	Tmax, Tmin, Tm	0.93	0.67	0.64	0.83	1.24	0.93
ANN	Tmax, Tmin, Tm	0.93	0.65	0.51	0.84	1.20	0.9
GAM	Tmax, Tmin, Tm	0.92	0.69	0.52	0.83	1.23	0.93
Blaney-Criddle							
RF	Ws, Sshn, Tm, RHmin, elev	0.98	0.38	0.27	0.97	0.51	0.35
SVM	Ws, Sshn, Tm, RHmin, elev	0.99	0.30	0.29	0.97	0.49	0.34
ANN	Ws, Sshn, Tm, RHmin, elev	0.98	0.32	0.22	0.97	0.49	0.34
GAM	Ws, Sshn, Tm, RHmin, elev	0.97	0.39	0.29	0.94	0.71	0.51
Radiation-based							
Makkink	Rs, T	0.96	0.99	0.66	0.82	1.95	1.34
RF	Sshn, Tm, pm	0.96	0.53	0.4	0.89	0.99	0.71
SVM	Sshn, Tm, pm	0.96	0.52	0.46	0.88	1.03	0.74
ANN	Sshn, Tm, pm	0.95	0.58	0.4	0.89	1.00	0.73
GAM	Sshn, Tm, pm	0.95	0.52	0.45	0.88	1.03	0.75
Jensen–Haise							
RF	Rs, T	0.94	8.86	6.71	0.88	8.81	6.85
SVM	Sshn, Tm	0.93	0.64	0.48	0.84	1.21	0.89
ANN	Sshn, Tm	0.94	0.61	0.49	0.86	1.24	0.84
GAM	Sshn, Tm	0.94	0.61	0.46	0.87	1.20	0.82
Priestley–Taylor							
RF	Rn, T	0.91	1.57	1.18	0.79	1.41	1.02
SVM	Sshn, Tm, pm, Tmax, Tmin, RHm	0.95	0.55	0.4	0.92	0.86	0.61
ANN	Sshn, Tm, pm, Tmax, Tmin, RHm	0.96	0.47	0.46	0.89	0.97	0.62
GAM	Sshn, Tm, pm, Tmax, Tmin, RHm	0.95	0.55	0.36	0.90	0.93	0.67
Abteu	Rs, Tmax	0.96	0.49	0.37	0.89	0.92	0.71
RF	Tmax, Sshn	0.93	0.78	0.57	0.82	2.76	1.14
SVM	Tmax, Sshn	0.92	0.71	0.52	0.83	1.27	0.94
ANN	Tmax, Sshn	0.93	0.67	0.53	0.85	1.18	0.87
GAM	Tmax, Sshn	0.93	0.66	0.51	0.85	1.15	0.85
Irmak	Tmax, Sshn	0.93	0.67	0.51	0.85	1.17	0.87
RF	Rs, T	0.94	1.12	1.26	0.86	2.05	1.45
SVM	Tm, Sshn	0.93	0.64	0.48	0.84	1.21	0.89
ANN	Tm, Sshn	0.94	0.61	0.49	0.86	1.13	0.84
GAM	Tm, Sshn	0.94	0.61	0.46	0.87	1.10	0.82
Mass transfer-based							
Penman	Ws, es-es	0.94	0.62	0.47	0.86	1.11	0.83
RF	Ws, VPD	0.89	8.11	7.13	0.05	4.17	17.36
SVM	Ws, VPD	0.89	0.87	0.65	0.18	2.86	2.28
ANN	Ws, VPD	0.88	0.86	0.63	0.27	2.64	2.13
GAM	Ws, VPD	0.89	0.82	0.61	0.28	2.60	2.15
GAM	Ws, VPD	0.94	0.59	0.45	0.27	2.60	2.16

Table 4 (continued)

Models	Models Input	R ²		RMSE		MAE	
		Monthly	Daily	Monthly	Daily	Monthly	Daily
WMO	Ws, es-ea	0.27	2.62	1.99	0.16	3.58	2.8
RF	Ws, VPD	0.89	0.87	0.65	0.18	2.86	2.28
SVM	Ws, VPD	0.88	0.86	0.63	0.27	2.64	2.13
ANN	Ws, VPD	0.89	0.82	0.61	0.28	2.60	2.15
GAM	Ws, VPD	0.94	0.59	0.45	0.27	2.60	2.16
Combined							
Valianlzas1	Rs, T, RH	0.96	0.55	0.4	0.89	1.39	0.97
RF	Tm, Sshn, RHm	0.98	0.33	0.44	0.88	1.04	0.75
SVM	Tm, Sshn, RHm	0.99	0.62	0.47	0.88	1.04	0.75
ANN	Tm, Sshn, RHm	0.99	0.25	0.44	0.88	1.02	0.74
GAM	Tm, Sshn, RHm	0.98	0.34	0.46	0.88	1.06	0.76
Valianlzas2	Rs, T, Tmin	0.95	0.53	0.37	0.87	1.33	0.9
RF	Tm, Tmin, Sshn	0.93	0.64	0.5	0.87	1.02	0.81
SVM	Tm, Tmin, Sshn	0.93	0.65	0.51	0.87	1.10	0.81
ANN	Tm, Tmin, Sshn	0.94	0.59	0.47	0.88	1.06	0.78
GAM	Tm, Tmin, Sshn	0.93	0.63	0.46	0.87	1.09	0.82
Valianlzas3	Rs, T, RH, Ws	0.98	1.27	0.97	0.96	1.24	0.95
RF	Tm, RHm, Ws, Sshn	0.94	0.61	0.27	0.97	0.52	0.36
SVM	Tm, RHm, Ws, Sshn	0.95	0.54	0.29	0.96	0.53	0.37
ANN	Tm, RHm, Ws, Sshn	0.98	0.32	0.23	0.97	0.52	0.36
GAM	Tm, RHm, Ws, Sshn	0.97	0.43	0.32	0.94	0.74	0.54
Doorenbos and Pruitt	Rn, Ws, VPD,	0.68	14.39	11.31	0.47	11.99	9.49
RF	Sshn, Tm, pm, RHm, Ws, VPD	0.97	0.37	0.27	0.97	0.48	0.33
SVM	Sshn, Tm, pm, RHm, Ws, VPD	0.97	0.44	0.29	0.97	0.47	0.33
ANN	Sshn, Tm, pm, RHm, Ws, VPD	0.98	0.29	0.21	0.97	0.48	0.33
GAM	Sshn, Tm, pm, RHm, Ws, VPD	0.97	0.35	0.27	0.94	0.71	0.52

with the Abteu model demonstrated superior accuracy compared to the other models. Notably, both of these models relied on radiation as a key input. These findings correspond with those of similar studies conducted by Heramb et al. (2023), Ünés et al. (2020), and Pendey et al. (2016), in which radiation-based models consistently demonstrated better performances.

Extensive research has consistently demonstrated the superior performance of ML models over empirical methods, a trend that was also observed in the present study. For example, Salam et al. (2020) reported the superiority of various ML models over empirical models (e.g., Ritchie, Thornthwaite, and Valiantzas) in predicting ET_0 . Mehdizadeh et al. (2017) showed that ML models (SVM, GEP, and MARS) consistently outperformed empirical methods in estimating ET_0 across 44 meteorological stations in Iran. Additionally, Alazba et al. (2016) employed the temperature-based Hargreaves model and the radiation-based Priestley-Taylor model to estimate ET_0 using local meteorological data; they found that the ML-based model yielded the most accurate results among all the approaches considered.

3.4 Variable Importance in ML Models for ET Estimation

Figure 8 illustrates the ten most important variables in ML models for estimating daily and monthly ET_0 . In the ANN model, T_m was the most important for both daily and monthly scales, followed by W_s for the monthly scale and RH_m for the daily scale. In the GAM model, variables such as P_m , VPD , and T_m had the most substantial impact on both temporal scales, with W_s being the third influential factor for the daily scale. As for the RF model, W_s emerged as the most important for both scales, followed by $Sshn$ for the daily scale and P_m for the monthly scale. Similarly in the SVM model, temperature exhibited the greatest effect on both temporal scales. In the daily scale, the three primary variables were T_m , T_{min} , and T_{max} , which aligns with the findings of Wu et al. (2019), who studied eight ML models with daily temperature and precipitation data from 14 different weather stations in China. The researchers recommended SVM models be used with temperature data only to predict daily ET_0 throughout China. Additionally, Yunfei et al. (2023) identified temperature and humidity as the most important factors in estimating ET in arid regions.

In monthly estimations, the variable T_m appeared most frequently with four repetitions, followed by W_s and P_m , each with two repetitions. Additionally, T_{max} , $Sshn$, and precipitation 24 hour (P_{24}) were deemed important, each with one repetition. For daily scale estimations, T_m was the most frequently repeated variable, followed by T_{max} and W_s . T_{min} , $Sshn$, and VPD variables were also considered important. Overall, it can be concluded that T_m , W_s , VPD , and $Sshn$ had the most important impact on forecasting, highlighting their importance in ET estimation.

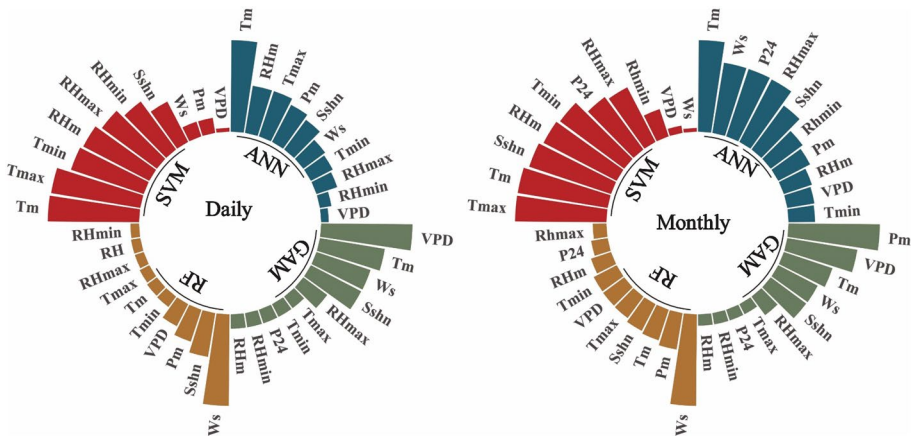


Fig. 8 Variable importance for ET estimation using ML models

4 Conclusion

The present study assessed the accuracy of thirteen experimental methods and four ML models for daily and monthly ET_0 estimation during drought, wet, and normal years and compared their performances against the FAO56-PM method, which served as a benchmark model. The study aimed to identify those variables that impact ET_0 estimation notably. The experimental models were categorized into four groups, among which the combined methods exhibited the best performances, while methods based on mass transfer demonstrated weaker performances. Notably, the performance of the experimental models varied across different time intervals. Consequently, the Valiantzas-3, Valiantzas-1, Abtew, Makkink, and Jensen-Haise models were identified as more suitable for monthly scale ET_0 estimation. For daily scale ET_0 estimation, however, the Valiantzas-3, Blaney-Criddle, Valiantzas-2, and Priestley-Taylor models were considered more appropriate. For cases with minimal input, the Abtew and Makkink models are recommended for monthly scale, while the Valiantzas-2 and Priestley-Taylor models are suggested for daily scale estimations. Nevertheless, the ML and FAO-56PM models performed similarly and exhibited comparable accuracy on both daily and monthly scales. Overall, SVM showed higher accuracy at the monthly scale, while ANN performed better at the daily scale. Furthermore, both ANN and SVM achieved better accuracy when using fewer variables, whereas RF had greater accuracy with a larger number of variables.

In sum, our findings indicate that T_m , W_s , and S_{shn} contribute positively to enhancing the accuracy of ML models, and ML models can serve as an alternative to the FAO56-PM method. Additionally, with similar inputs, ML models outperformed experimental methods in both daily and monthly scales. In general, T_m , W_s , VPD, and S_{shn} were found to have the most significant influence on predicting ET_0 . The present study was conducted in arid and semi-arid regions of Iran. Therefore, it is recommended this research be replicated under different climatic conditions to assess the applicability and performance of this research in diverse regions.

Supplementary Information The online version contains supplementary material available at <https://doi.org/10.1007/s11269-023-03670-2>.

Data Availability Data will be made available on request.

Declarations

Ethical Approval Not required as no animal/human was involved in the study.

Consent to Participate Authors agree to participate any survey or feedback tasks.

Consent to Publish Authors consent publication of the manuscript to the journal publisher.

Competing Interests There is no competing interest in regard to the study.

References

- Abd-Elaty I, Kushwaha NL, Patel A (2023) Novel Hybrid Machine Learning Algorithms for Lakes Evaporation and Power Production using Floating Semitransparent Polymer Solar Cells. *Water Resour Manage* 37:4639–4661. <https://doi.org/10.1007/s11269-023-03565-2>
- Abtew W (1996) Evapotranspiration measurements and modeling for three wetland systems in South Florida 1. *JAWRA* 32(3). <https://doi.org/10.1111/j.1752-1688.1996.tb04044.x>

- Alazba A, Yassin M, Mattar M (2016) Modeling daily evapotranspiration in hyper-arid environment using gene expression programming. *Arab J Geosci* 9:202. <https://doi.org/10.1007/s12517-015-2273-x>
- Alizadeh A, Keshavarz A (2005) Status of agricultural water use in Iran. In *Water conservation, reuse, and recycling: Proceedings of an Iranian-American workshop* 4:94–105. Washington DC, USA: National Academies Press
- Allen RG, Pereira LS, Raes D, Smith M (1998) *Crop evapotranspiration-Guidelines for computing crop water requirements-FAO Irrigation and drainage paper* 56. Fao Rome 300(9):D05109
- Almorox J, Quej VH, Marti P (2015) Global performance ranking of temperature-based approaches for evapotranspiration estimation considering Köppen climate classes. *J Hydrol* 528:514–522. <https://doi.org/10.1016/j.jhydrol.2015.06.057>
- Amani S, Shafizadeh-Moghadam H (2023) A review of machine learning models and influential factors for estimating evapotranspiration using remote sensing and ground-based data. *Agric Water Manag* 284:108324
- Anderson MC, Norman JM, Mecikalski JR, Otkin JA, Kustas WP (2007) A climatological study of evapotranspiration and moisture stress across the continental United States based on thermal remote sensing: 1. Model formulation. *J Geophys Res Atmos* 112(D10). <https://doi.org/10.1029/2006JD007506>
- Bachour R, Maslova I, Ticlavilca AM, Walker WR, McKee M (2016) Wavelet-multivariate relevance vector machine hybrid model for forecasting daily evapotranspiration. *Stoch Environ Res Risk Assess* 30:103–117. <https://doi.org/10.1007/s00477-015-1039-z>
- Bellido-Jiménez JA, Estévez J, García-Marín AP (2021) New machine learning approaches to improve reference evapotranspiration estimates using intra-daily temperature-based variables in a semi-arid region of Spain. *Agric Water Manag* 245:106558. <https://doi.org/10.1016/j.agwat.2020.106558>
- Blaney HF, Criddle WD (1962) Determining consumptive use and irrigation water requirements. US Department of Agriculture
- Breiman L (2001) Random forests. *Mach Learn* 45:5–32. <https://doi.org/10.1023/A:1010933404324>
- Carter C, Liang S (2019) Evaluation of ten machine learning methods for estimating terrestrial evapotranspiration from remote sensing. *Int J Appl Earth Obs Geoinf* 78:86–92. <https://doi.org/10.1016/j.jag.2019.01.020>
- Chow V, Maidment DR, Mays LW (1971) *Applied hydrology*. McGraw-Hill Series in Water Resources and Environmental Engineering. McGraw-Hill: New York. ISBN 0–07–010810–2
- Chu R, Li M, Shen S, Islam AR, Cao W, Tao S, Gao P (2017) Changes in reference evapotranspiration and its contributing factors in Jiangsu, a major economic and agricultural province of eastern China. *Water* 9(7):486. <https://doi.org/10.3390/w9070486>
- Cortes C, Vapnik V (1995) Support-vector networks. *Mach Learn* 20(3):273–297
- De Paola F, Giugni M (2013) Coupled spatial distribution of rainfall and temperature in USA. *Procedia Environ Sci* 19:178–187. <https://doi.org/10.1016/j.proenv.2013.06.020>
- Doorenbos J, Pruitt WO (1977) *Crop water requirements. FAO irrigation and drainage, vol 24. Land and Water Development Division, FAO, Rome, pp 1–144*
- Eccel E (2012) Estimating air humidity from temperature and precipitation measures for modelling applications. *Meteorol Appl* 19(1):118–128. <https://doi.org/10.1002/met.258>
- Elbeltagi A, Kumari N, Dharpure JK, Mokhtar A, Alsafadi K, Kumar M, Mehdinejadiani B, Ramezani Etedali H, Brouziyne Y, Towfiqul Islam AR, Kuriqi A (2021) Prediction of combined terrestrial evapotranspiration index (CTEI) over large river basin based on machine learning approaches. *Water* 13(4):547. <https://doi.org/10.3390/w13040547>
- Fan J, Guyot A, Ostergaard KT, Lockington DA (2018) Effects of earlywood and latewood on sap flux density-based transpiration estimates in conifers. *Agric For Meteorol* 249:264–274
- Fan J, Ma X, Wu L, Zhang F, Yu X, Zeng W (2019) Light Gradient Boosting Machine: An efficient soft computing model for estimating daily reference evapotranspiration with local and external meteorological data. *Agric Water Manag* 225:105758. <https://doi.org/10.1016/j.agwat.2019.105758>
- Fathi-Taperasht A, Shafizadeh-Moghadam H, Minaei M, Xu T (2022) Influence of drought duration and severity on drought recovery period for different land cover types: evaluation using MODIS-based indices. *Ecol Ind* 141:109146. <https://doi.org/10.1016/j.ecolind.2022.109146>
- Feng Y, Cui N, Zhao L, Hu X, Gong D (2016) Comparison of ELM, GANN, WNN and empirical models for estimating reference evapotranspiration in humid region of Southwest China. *J Hydrol* 536:376–383. <https://doi.org/10.1016/j.jhydrol.2016.02.053>
- Feng Y, Peng Y, Cui N, Gong D, Zhang K (2017) Modeling reference evapotranspiration using extreme learning machine and generalized regression neural network only with temperature data. *Comput Electron Agric* 136:71–78. <https://doi.org/10.1016/j.compag.2017.01.027>
- Ferreira LB, da Cunha FF, de Oliveira RA (2019) Fernandes Filho EI. Estimation of reference evapotranspiration in Brazil with limited meteorological data using ANN and SVM—A new approach. *J Hydrol* 572:556–70. <https://doi.org/10.1016/j.jhydrol.2019.03.028>

- Hargreaves GH, Samani ZA (1985) Reference crop evapotranspiration from temperature. *Appl Eng Agric* 1(2):96–99. <https://doi.org/10.13031/2013.26773>
- Hargreaves GL, Hargreaves GH, Riley JP (1985) Irrigation water requirements for Senegal River basin. *J Irrig Drain Eng* 111(3):265–275. [https://doi.org/10.1061/\(ASCE\)0733-9437\(1985\)111:3\(265\)](https://doi.org/10.1061/(ASCE)0733-9437(1985)111:3(265))
- Hastie TJ, Tibshirani R (1990) Generalized additive models. Chapman & Hall, London, p 352
- Hastie T, Tibshirani R, Friedman J (2009) "Random forests." The elements of statistical learning. Springer, New York, NY, 2009. 587–604. <https://link.springer.com/book/10.1007/978-0-387-84858-7>
- Hecht-Nielsen R (1992) Theory of the backpropagation neural network. *Neural networks for perception*. Academic Press, pp 65–93
- Heramb P, Ramana Rao KV, Subeesh A, Srivastava A (2023) Predictive modelling of reference evapotranspiration using machine learning models coupled with grey wolf optimizer. *Water* 15(5):856. <https://doi.org/10.3390/w15050856>
- Holmes JW (1984) Measuring evapotranspiration by hydrological methods. *Agric Water Manag* 8(1–3): 29–40. [https://doi.org/10.1016/0378-3774\(84\)90044-1](https://doi.org/10.1016/0378-3774(84)90044-1)
- Irmak S, Irmak A, Allen RG, Jones JW (2003) Solar and net radiation-based equations to estimate reference evapotranspiration in humid climates. *J Irrig Drain Eng* 129(5):336–347. [https://doi.org/10.1061/\(ASCE\)0733-9437\(2003\)129:5\(336\)](https://doi.org/10.1061/(ASCE)0733-9437(2003)129:5(336))
- Islam S, Alam AR (2021) Performance evaluation of FAO Penman-Monteith and best alternative models for estimating reference evapotranspiration in Bangladesh. *Heliyon* 7(7):e07487. <https://doi.org/10.1016/j.heliyon.2021.e07487>
- Jensen ME, Haise HR (1963) Estimating evapotranspiration from solar radiation. *J Irrig Drain Div* 89(4):15–41. <https://doi.org/10.1061/JRCEA4.0000287>
- Jovic S, Nedeljkovic B, Golubovic Z, Kostic N (2018) Evolutionary algorithm for reference evapotranspiration analysis. *Comput Electron Agric* 150:1–4. <https://doi.org/10.1016/j.compag.2018.04.003>
- Kisi O, Sanikhani H, Zounemat-Kermani M, Niazi F (2015) Long-term monthly evapotranspiration modeling by several data-driven methods without climatic data. *Comput Electron Agric* 115:66–77. <https://doi.org/10.1016/j.compag.2015.04.015>
- Krishnashetty PH, Balasangameshwara J, Sreeman S, Desai S, Kantharaju AB (2021) Cognitive computing models for estimation of reference evapotranspiration: A review. *Cogn Syst Res* 70:109–116. <https://doi.org/10.1016/j.cogsys.2021.07.012>
- Küçüktopcu E, Cemek E, Cemek B, Simsek H (2023) Hybrid Statistical and Machine Learning Methods for Daily Evapotranspiration Modeling. *Sustainability* 15(7):5689. <https://doi.org/10.3390/su15075689>
- Kumar M, Raghuwanshi NS, Singh R, Wallender WW, Pruitt WO (2002) Estimating evapotranspiration using artificial neural network. *J Irrig Drain Eng* 128(4):224–233. [https://doi.org/10.1061/\(ASCE\)0733-9437\(2002\)128:4\(224\)](https://doi.org/10.1061/(ASCE)0733-9437(2002)128:4(224))
- Landeras G, Bekoe E, Ampof J, Logah F, Diop M, Cisse M, Shiri J (2018) New alternatives for reference evapotranspiration estimation in West Africa using limited weather data and ancillary data supply strategies. *Theor Appl Climatol* 132:701–716. <https://doi.org/10.1007/s00704-017-2120-y>
- Li Y, Qin Y, Rong P (2022) Evolution of potential evapotranspiration and its sensitivity to climate change based on the Thornthwaite, Hargreaves, and Penman-Monteith equation in environmental sensitive areas of China. *Atmos Res* 273:106178. <https://doi.org/10.1016/j.atmosres.2022.106178>
- Liu X, Xu C, Zhong X, Li Y, Yuan X, Cao J (2017) Comparison of 16 models for reference crop evapotranspiration against weighing lysimeter measurement. *Agric Water Manag* 184:145–155. <https://doi.org/10.1016/j.agwat.2017.01.017>
- Lu Y, Li T, Hu H, Zeng X (2023) Short-term prediction of reference crop evapotranspiration based on machine learning with different decomposition methods in arid areas of China. *Agric Water Manag* 279:108175. <https://doi.org/10.1016/j.agwat.2023.108175>
- Makkink GF (1957) Testing the Penman formula by means of lysimeters. *Proc Inst Civ Eng* 11:277–288
- Mantero P, Moser G, Serpico SB (2005) Partially supervised classification of remote sensing images through SVM-based probability density estimation. *IEEE Trans Geosci Remote Sens* 43(3):559–570
- McCuen RH (2016) Modeling hydrologic change: statistical methods. CRC Press
- Mehdizadeh S, Behmanesh J, Khalili K (2017) Using MARS, SVM, GEP and empirical equations for estimation of monthly mean reference evapotranspiration. *Comput Electron Agric* 139:103–114. <https://doi.org/10.1016/j.compag.2017.05.002>
- Mohammadrezapour O, Piri J, Kisi O (2018) Comparison of SVM, ANFIS and GEP in modeling monthly potential evapotranspiration in an arid region (Case study: Sistan and Baluchestan Province, Iran). *Water Supply* 19(2):392–403. <https://doi.org/10.2166/ws.2018.084>
- Mousavi R, Sabziparvar AA, Marofi S, Ebrahimi Pak NA, Heydari M (2015) Calibration of the Angström-Prezscott solar radiation model for accurate estimation of reference evapotranspiration in the absence of observed solar radiation. *Theor Appl Climatol* 119:43–54. <https://doi.org/10.1007/s00704-013-1086-7>

- O'Brien RM, (2007) A caution regarding rules of thumb for variance inflation factors. *Qual Quant* 41:673–90. <https://doi.org/10.1007/s11135-006-9018-6>
- Pandey PK, Dabral PP, Pandey V (2016) Evaluation of reference evapotranspiration methods for the northeastern region of India. *ISWCR* 1:52–63. <https://doi.org/10.1016/j.iswcr.2016.02.003>
- Penman HL (1948) Natural evaporation from open water, bare soil and grass. *Proc R Soc Lon Ser A Math Phys* 193(1032):120–45. <https://doi.org/10.1098/rspa.1948.0037>
- Priestley CH, Taylor RJ (1972) On the assessment of surface heat flux and evaporation using large-scale parameters. *MWR* 100(2):81–92. [https://doi.org/10.1175/1520-0493\(1972\)100%3C0081:OTAOSH%3E2.3.CO;2](https://doi.org/10.1175/1520-0493(1972)100%3C0081:OTAOSH%3E2.3.CO;2)
- Rahimi khoob A (2008) Artificial neural network estimation of reference evapotranspiration from pan evaporation in a semi-arid environment. *Irrig Sci* 27:35–39. <https://doi.org/10.1007/s00271-008-0119-y>
- Rashid Niaghi A, Hassanijalilian O, Shiri J (2021) Estimation of reference evapotranspiration using spatial and temporal machine learning approaches. *Hydrology* 8(1):25. <https://doi.org/10.3390/hydrology8010025>
- Roy DK, Sarkar TK, Biswas SK (2023) Generalized Daily Reference Evapotranspiration Models Based on a Hybrid Optimization Algorithm Tuned Fuzzy Tree Approach. *Water Resour Manage* 37:193–218. <https://doi.org/10.1007/s11269-022-03362-3>
- Rumelhart DE, Hinton GE, Williams RJ (1986) Learning representations by back-propagating errors. *Nature* 323(6088):533–536
- Salam R, Islam AR (2020) Potential of RT, Bagging and RS ensemble learning algorithms for reference evapotranspiration prediction using climatic data-limited humid region in Bangladesh. *J Hydrol* 590:125241. <https://doi.org/10.1016/j.jhydrol.2020.125241>
- Scanlon BR, Tyler SW, Wierenga PJ (1997) Hydrologic issues in arid, unsaturated systems and implications for contaminant transport. *Rev Geophys* 35(4):461–490. <https://doi.org/10.1029/97RG01172>
- Shan X, Cui N, Cai H, Hu X, Zhao L (2020) Estimation of summer maize evapotranspiration using MARS model in the semi-arid region of northwest China. *Comput Electron Agric* 174:105495. <https://doi.org/10.1016/j.compag.2020.105495>
- Shi L, Feng P, Wang B, Li Liu D, Cleverly J, Fang Q, Yu Q (2020) Projecting potential evapotranspiration change and quantifying its uncertainty under future climate scenarios: A case study in south-eastern Australia. *J Hydrol* 584:124756. <https://doi.org/10.1016/j.jhydrol.2020.124756>
- Tabari H, Kisi O, Ezani A, Talaei PH (2012) SVM, ANFIS, regression and climate based models for reference evapotranspiration modeling using limited climatic data in a semi-arid highland environment. *J Hydrol* 444:78–89. <https://doi.org/10.1016/j.jhydrol.2012.04.007>
- Teuling AJ, Hirschi M, Ohmura A, Wild M, Reichstein M, Ciais P, Buchmann N, Ammann C, Montagnani L, Richardson AD, Wohlfahrt G (2009) A regional perspective on trends in continental evaporation. *Geophys Res Lett* 36(2). <https://doi.org/10.1029/2008GL036584>
- Üneş F, Kaya YZ, Mamak M (2020) Daily reference evapotranspiration prediction based on climatic conditions applying different data mining techniques and empirical equations. *Theor Appl Climatol* 141:763–773. <https://doi.org/10.1007/s00704-020-03225-0>
- Valiantzas JD (2013a) Simple ET 0 forms of Penman's equation without wind and/or humidity data. I: Theoretical development. *J Irrig Drain Eng* 139(1):1–8. [https://doi.org/10.1061/\(ASCE\)IR.1943-4774.0000520](https://doi.org/10.1061/(ASCE)IR.1943-4774.0000520)
- Valiantzas JD (2013b) Simple ET 0 forms of Penman's equation without wind and/or humidity data. II: Comparisons with reduced set-FAO and other methodologies. *J Irrig Drain Eng* 139(1):9–19. [https://doi.org/10.1061/\(ASCE\)IR.1943-4774.0000502](https://doi.org/10.1061/(ASCE)IR.1943-4774.0000502)
- Wang S, Lian J, Peng Y, Hu B, Chen H (2019) Generalized reference evapotranspiration models with limited climatic data based on random forest and gene expression programming in Guangxi, China. *Agric Water Manag* 221:220–230. <https://doi.org/10.1016/j.agwat.2019.03.027>
- Wen X, Si J, He Z, Wu J, Shao H, Yu H (2015) Support-vector-machine-based models for modeling daily reference evapotranspiration with limited climatic data in extreme arid regions. *Water Resour Manag* 29:3195–3209. <https://doi.org/10.1007/s11269-015-0990-2>
- WMO (1963) Sites for wind-power installations; WMO No. 156, Technical Note No. 63. WMO, Geneva, Switzerland. https://library.wmo.int/index.php?lvl=notice_display&id=5475#_YjfmEHpBzDc. Accessed 8 Feb 2022
- Wu L, Zhou H, Ma X, Fan J, Zhang F (2019) Daily reference evapotranspiration prediction based on hybridized extreme learning machine model with bio-inspired optimization algorithms: Application in contrasting climates of China. *J Hydrol* 577:123960. <https://doi.org/10.1016/j.jhydrol.2019.123960>
- Yan X, Yang N, Ao R, Mohammadian A, Liu J, Cao H, Yin P (2023) Deep learning for daily potential evapotranspiration using a HS-LSTM approach. *Atmos Res* 10:106856. <https://doi.org/10.1016/j.atmosres.2023.106856>

Yunfei L, Dongwei G, Changjun Y (2023) Estimating the temporal and spatial variations in evapotranspiration with a nonlinear evaporation complementary relationship model in hyper-arid areas. *Water Resour Manage* 37:521–535. <https://doi.org/10.1007/s11269-022-03384-x>

Publisher's Note Springer Nature remains neutral with regard to jurisdictional claims in published maps and institutional affiliations.

Springer Nature or its licensor (e.g. a society or other partner) holds exclusive rights to this article under a publishing agreement with the author(s) or other rightsholder(s); author self-archiving of the accepted manuscript version of this article is solely governed by the terms of such publishing agreement and applicable law.